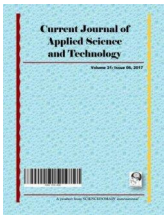

Current Journal of Applied Science and Technology

27(1): 1-11, 2018; Article no.CJAST.40125
ISSN: 2457-1024
(Past name: British Journal of Applied Science & Technology, Past ISSN: 2231-0843, NLM ID: 101664541)

The Coupling Conduction Effects on Natural Convection Flow along a Vertical Flat Plate with Joule Heating and Heat Generation

Md. M. Alam[1], Md. Saddam Hossain[1], M. M. Parvez[1*] and Irin Rahman[1]

[1]Department of Mathematics, Dhaka University of Engineering and Technology, Gazipur, Bangladesh.

Authors' contributions

This work was carried out in collaboration between all authors. Authors MMA and MSH designed the study, performed the statistical analysis, wrote the protocol and wrote the first draft of the manuscript. Authors MMA and MMP managed the analyses of the study. Authors MMP and IR managed the literature searches. All authors read and approved the final manuscript.

Article Information

DOI: 10.9734/CJAST/2018/40125
Editor(s):
(1) Pengtao Sun, Associate Professor, University of Nevada Las Vegas,4505 Maryland Parkway, USA.
Reviewers:
(1) Abdul Maleque, American International University, Bangladesh.
(2) Animasaun, L. Isaac, Federal University of Technology, Nigeria.
(3) Bhim Sen Kala, Doon University, India.
Complete Peer review History: http://www.sciencedomain.org/review-history/24214

Original Research Article

Received 24th January 2018
Accepted 3rd April 2018
Published 19th April 2018

ABSTRACT

The out-turn of heat generation and Joule heating on natural convection flow through a vertical flat plate have been investigated in the given article. Joule heating and heat conduction due to wall thickness 'b' are esteemed as well in this analysis. With the intent to obtain similarity solutions to the problem being constituted, the evolved equations are made dimensionless employing appropriate transformations. The non-dimensional equations are then modified into non-linear equations by bringing into being a non-similarity transformation. The out-turn non-linear alike equations confine with their commensurate boundary conditions formed on conduction and convection are solved numerically applying the finite difference method accompanied by Newton's linearization approximation. The numerical outcomes in terms of the skin friction coefficient, velocity, temperature, and surface temperature profiles are shown both graphically and in tabular forms for the different values of the parameters correlated with the problem.

**Corresponding author: E-mail: mmparvez@duet.ac.bd;*

Keywords: Natural convection; Joule heating; heat generation and Prandtl's number; magneto-hydrodynamics.

1. INTRODUCTION

Free convection flow is often envisaged in cooling of nuclear reactors or in the study of the structure of stars and planets. Along with the free convection flow the phenomenon of the boundary layer flow of an electrically conducting fluid to a vertical flat plate in existence of Joule-heating, magnetic field and heat generation are also very common, because of their applications in nuclear engineering in conjunction with the cooling of reactors. Natural convection heat transfer has attracted a considerable attention because of its widespread applications in the areas of energy conservations cooling of electrical and electronics components, the design of solar collectors, heat exchangers and so on. The main difficulty facing the solution to natural convection problems lies in the determination of the velocity field which greatly influences the heat transfer process. El-Amin [1] studied conjugate effects of viscous dissipation and Joule heating on MHD forced convection through a nonisothermal horizontal cylinder embedded in a fluid-saturated porous medium. Gebhart [2] also investigated the results of viscous dissipation in a natural flow. Alam et al. [3] studied the consequences of pressure stress work and viscous dissipation in natural convection flow towards a vertical flat plate with heat conduction. Joule heating effects on the coupling of conduction on MHD free convection flow from a vertical flat plate have been investigated by Alim et al. [4]. Vajravelu et al. [5] examined the effects of heat transfer in a viscous fluid on a stretching sheet with viscous dissipation and internal heat generation. Hossain [6] analyzed the viscous and Joule heating sequels on MHD natural convection flow with a variable plate temperature. Hossain et al. [7] investigated the effects of free convection flow along a perpendicular wavy surface temperature associated with heat generation/absorption. Miyamoto et al. [8] considered the effect of axial heat conduction in a vertical flat plate on free convection heat transfer. Molla et al. [9] performed the effects of magneto-hydrodynamic natural convection flow on a sphere in presence of heat generation. Pozzi and Lupo [10] studied the coupling of conduction with laminar natural convection along a flat plate. A numerical method in boundary layer theory has been investigated by Keller, H B. [11]. Physical and Computational Aspects of Convective Heat Transfer have been discussed FORTRAN Programmed by Cebeci, T. et al. [12]. Effects of conduction variation on MHD free convection flow along a vertical plane plate are considered by Shafiqul Islam et al. [13]. Chowdhury, et al. [14], performed the MHD free convection flow of viscoelastic fluid past an infinite porous plate. Hossain, M. A. [15] studied the effects of Viscous and Joule heating effects on MHD free convection flow with variable plate temperature, Hossain MA. et al. [16] have been investigated the MHD forced and free convection boundary layer flow along a vertical porous plate, The present investigation is mainly concerned with the yielding of Joule heating on natural convection flow along a perpendicular flat plate with heat generation in the entire region from upstream to downstream of a viscous incompressible and electrically conducting fluid. It deals with the upshot of Joule heating parameter *Jul*, the Prandtl's number *Pr* and the heat generation parameter *Q* over the velocity and temperature fields as well as on the skin friction and surface temperature. In the following sections, the detailed derivations of the governing equations for the flow are discussed.

2. GOVERNING EQUATIONS OF THE FLOW

It has been considered that the steady two-dimensional laminar natural convection boundary layer flow of a viscous incompressible electrically conducting fluid along a side of a vertical flat plate of thickness '*b*' insulated on the edges with temperature T_b being maintained on the other side in the presence of a uniformly distributed transverse magnetic field. The flow aspect and the coordinates system are sighted in Fig. 1.

With the mathematical statement of the basic conservation acts of mass, momentum, and energy for the steady viscous incompressible and electrically conducting flow, after simplifying we have

$$\frac{\partial U}{\partial X}+\frac{\partial V}{\partial Y}=0 \tag{1}$$

$$U\frac{\partial U}{\partial X}+V\frac{\partial U}{\partial Y}=\nu\frac{\partial^2 U}{\partial Y^2} +g\beta\left(T_f-T\infty\right)-\frac{\sigma H_0^2 U}{\nu} \tag{2}$$

$$U\frac{\partial T}{\partial X}+V\frac{\partial T}{\partial Y}=\frac{K}{\rho C_P}\frac{\partial^2 T}{\partial Y^2}+\frac{\sigma B_0^2}{\rho C_P}U^2+\frac{Q_0}{\rho C_P}\left(T_f-T_\infty\right) \quad (3)$$

Where, U and V are the velocity components towards the X and Y axis respectively, T is the fluid temperature and T_∞ is the ambient fluid temperature in the boundary layer, g is the gravitational acceleration, is the thermal conductivity, ρ is the density, C_p is the specific heat constant pressure and ν is the kinematic viscosity. The sum of heat generated or absorbed per unit volume is $Q_0(T-T_\infty)$, Q_0 being either positive or negative constant. The source term describes the heat generation when $Q_0 > 0$ and the heat absorption when $Q_0 < 0$. In the energy equation, heat generation and Joule heating terms are included. Here for exterior conditions we know, $\partial P/\partial X=\rho_e g$ and $\rho=\rho_e$, P is the pressure, H_0 is the magnetic field strength and σ is the electric conductivity.

The appropriate boundary conditions to be given below

$$\begin{aligned}&U=0,\ V=0, T_f=(X,0) \quad \text{at}\\ &Y=0,\ X\rangle 0,\\ &U\to 0, T_f\to T_\infty \ \text{as}\ Y\to\infty, X\rangle 0\end{aligned} \quad (4)$$

The temperature and the heat flux are considered continuous at the interface for the coupled conditions and at the interface, we must have

$$\frac{k_s}{k_f}\frac{\partial T_{so}}{\partial Y}=\left(\frac{\partial T_f}{\partial Y}\right)_{Y=0} \quad (5)$$

Where k_s and k_f are the thermal conductivity of the solid and the fluid respectively. The temperature T_{so} in the solid as given by A. Pozzi and M. Lupo is

$$T_{so}=T(X,0)-\{T_b-T(X,0)\}\frac{Y}{b} \quad (6)$$

Where $T(X,0)$ is the unknown temperature at the interface to be determined from the solutions of the equations.

We observe that the equations (1) - (3) together with the boundary conditions (4) - (5) are non-linear partial differential equations. In the following sections, the solution methods of these equations are discussed in details.

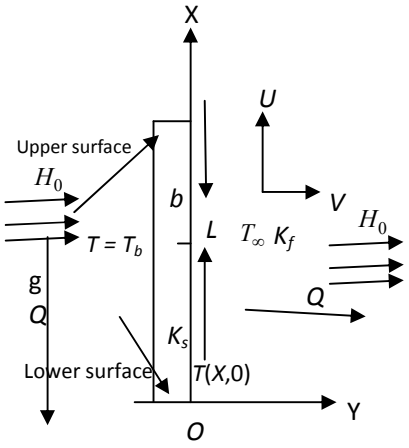

Fig. 1. Physical configuration and coordinates system

3. TRANSFORMATION OF THE GOVERNING EQUATIONS

Equations (1) – (3) may now be non-dimensionalized by using the following dimensionless dependent and independent variables:

$$\begin{aligned}&x=\frac{X}{L},\ y=\frac{Y}{L}d^{1/4},\ U=\frac{\nu}{L}d^{1/2}u,\\ &V=\frac{\nu}{L}d^{1/4}v,\ \theta=\frac{T_f-T_\infty}{T_b-T_\infty},\\ &L=\frac{\nu^{2/3}}{g^{1/3}},\ d=\beta(T_b-T_\infty)\end{aligned} \quad (7)$$

For the problem of natural convection, its parabolic character has no characteristic length; L has been defined in terms of ν and g, which are the intrinsic properties of the system. The reference length along the 'y' direction has been modified by a factor $d^{1/4}$ in order to eliminate this quantity from the dimensionless equations and the boundary conditions.

The magnetohydrodynamic field in the fluid is governed by the boundary layer equations, which in the non-dimensional form obtained by introducing the dimensionless variables described in (7), may be written as

$$\frac{\partial u}{\partial x}+\frac{\partial v}{\partial y}=0 \tag{8}$$

$$u\frac{\partial u}{\partial x}+v\frac{\partial u}{\partial y}+Mu=\frac{\partial^2 u}{\partial y^2}+\theta \tag{9}$$

$$u\frac{\partial \theta}{\partial x}+v\frac{\partial \theta}{\partial y}=\frac{1}{p_r}\frac{\partial^2 \theta}{\partial y^2} +u^2 Jul+Q\theta \tag{10}$$

Where, $Jul=\sigma B_0^2 \nu d^{1/2}\big/\rho C_p\left(T_b-T_\infty\right)$, the Joule-heating parameter, $M=\sigma H_0 L^2/\mu G_r^{\frac{1}{2}}$ is the dimensionless magnetic parameter, $\Pr=\mu C_p\big/\kappa_f$, the Prandtl's number and $Q_0 L^2\big/\mu C_P d^{1/2}=Q$, where Q is the heat generation parameter. The corresponding boundary conditions (4) - (6) take the following form:

$$u=v=0,\ \theta-1=p\left(\frac{\partial \theta}{\partial y}\right) \text{ at } y=0,\qquad u\to 0,\ \theta\to 0 \text{ as } y\to\infty \tag{11}$$

Where *p* is the conjugate conduction parameter given by $p=\left(\frac{k_f}{k_s}\right)\left(\frac{y}{L}\right)d^{\frac{1}{4}}$. Here, the coupling parameter '*p*' governs the described problem. The order of magnitude of '*p*' depends actually on, $b\big/L$, $k_f\big/k_s$ and $d^{\frac{1}{4}}$ being the order of unity. The term $b\big/L$ attains values much greater than one because of *L* is small. In case of air, $\left(\frac{k_f}{k_s}\right)$ becomes very small when the vertical plate is highly conductive i.e. $k_s \rangle\rangle 1$ and for materials, O $\left(\frac{k_f}{k_s}\right)$ = 0.1 such as glass. Therefore, in different cases '*p*' is different but not always a small number. In the present investigation, we have considered *p* = 1 which is accepted for $b\big/L$ of O $\left(\frac{k_f}{k_s}\right)$.

To solve the equations (9) and (10) are subjected to the boundary conditions (11), the following transformations are introduced for the flow region starting from upstream to downstream.

$$\begin{aligned} &u=\frac{\partial \psi}{\partial y}, v=-\frac{\partial \psi}{\partial x}\\ &\psi=x^{4/5}(1+x)^{-1/20}f(x,\eta),\\ &\eta=y\,x^{-1/5}(1+x)^{-1/20},\\ &\theta=x^{1/5}(1+x)^{-1/5}h \end{aligned} \tag{12}$$

Here η is the dimensionless similarity variable and ψ is the stream function which satisfies the equation of continuity and *h* (x,η) is the dimensionless temperature. Therefore, substituting these transformations into equations (9) and (10) and after simplifying, we get the following transformed non-dimensional equations.

$$\begin{aligned} &f'''+\frac{16+15x}{20(1+x)}ff''-\frac{6+5x}{10(1+x)}f'^2\\ &-Mx^{2/5}(1+x)^{1/10}f'+h=x\left(f'\frac{\partial f'}{\partial x}-f''\frac{\partial f}{\partial x}\right) \end{aligned} \tag{13}$$

$$\begin{aligned} &\frac{1}{\Pr}h''+\frac{16+15x}{20(1+x)}fh'-\frac{1}{5(1+x)}f'h\\ &+Jul\,x^{\frac{7}{5}}(1+x)^{-\frac{1}{2}}f'^2+Q\,x^{1/5}(1+x)^{-1/5}h\\ &=x\left(f'\frac{\partial h}{\partial x}-h'\frac{\partial f}{\partial x}\right) \end{aligned} \tag{14}$$

In the above equations, the primes denote differentiation with respect to η .

The boundary conditions (11) after simplifying, we have the following form

$$\begin{aligned} &f(x,0)=f'(x,0)=0,\\ &h(x,0)=-(1+x)^{1/4}\\ &+x^{1/5}(1+x)^{1/20}h(x,0)\\ &f'(x,\infty)=0, h'(x,\infty)=0 \end{aligned} \tag{15}$$

The solutions of the above equations (13) and (14) together with the boundary conditions (15) enable us to calculate the skin friction τ and the surface temperature θ at the surface in the boundary layer from the following relations:

$$\tau = \mu\left\{x^{2/5}(1+x)^{-3/20} f''(x,0)\right\} \quad (16)$$

$$\theta = \left\{x^{1/5}(1+x)^{-1/5} h(x,0)\right\} \quad (17)$$

4. METHOD OF SOLUTION

This paper regarding the free convection flow of viscous incompressible fluid towards a uniformly heated vertical flat plate in arrival of Joule heating and heat generation has been investigated using the very efficient implicit finite difference method known as the Keller box scheme developed by Keller [11], which is well documented by Cebeci and Bradshaw [12].

To apply the aforementioned method, Equations (13) and (14) with their boundary conditions (15) are first converted into the following system of first order equations. Here, *x* is replaced by ξ so that the coordinates are replaced by (ξ, η). For this purpose, we introduce new dependent variables $u(\xi,\eta)$, $v(\xi,\eta)$, $p(\xi,\eta)$ and $g(\xi,\eta)$ so that the transformed momentum and energy equations can be rewritten as

$$(x, \eta)$$

$$f' = u \quad (18)$$

$$u' = v \quad (19)$$

$$g' = p \quad (20)$$

$$v' + P_1 f\, u' - P_2 u^2 + g - P_3 f' = \xi\left(u\frac{\partial u}{\partial \xi} - v\frac{\partial f}{\partial \xi}\right) \quad (21)$$

$$\frac{1}{\mathrm{Pr}} p' + P_1 f\, p - P_4 u\, g + P_5 u^2 + P_6\, g = \xi\left(u\frac{\partial g}{\partial \xi} - p\frac{\partial f}{\partial \xi}\right) \quad (22)$$

Where $x = \xi,\ h = g$,

$$P_1 = \frac{16+15\xi}{20(1+\xi)} \quad , \quad P_2 = \frac{6+5\xi}{10(1+\xi)} \quad ,$$

$$P_3 = Mx^{2/5}(1+x)1/10 \,,$$

$$P_4 = \frac{1}{5(1+\xi)} \,,\ P_5 = Jul\ \xi^{\frac{7}{5}}(1+\xi)^{-\frac{1}{2}}$$

and $P_6 = Q\ \xi^{\frac{1}{5}}(1+\xi)^{-\frac{1}{5}}$

and the boundary conditions (15) are

$$\begin{aligned} &f(\xi,0) = 0, u(\xi,0) = 0, \\ &g(\xi,0) = -(1+\xi)^{\frac{1}{4}} \\ &+\xi^{\frac{1}{5}}(1+\xi)^{\frac{1}{20}} g(\xi,0) \\ &u(\xi,\infty) = 0, \quad p(\xi,\infty) = 0 \end{aligned} \quad (23)$$

Now, we consider the net rectangle on the (ξ, η) plane as shown in the Fig. 2 and denote the net points by

$$\begin{aligned} &\xi^0 = 0, \xi^n = \xi^{n-1} + k_n, \\ &n = 1,2,3,---,N, \eta_0 = 0, \\ &\eta_j = \eta_{j-1} + h_j,\ j = 1,2,3,---,J \end{aligned} \quad (24)$$

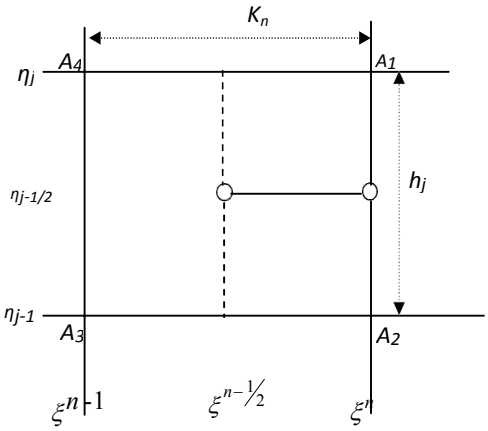

Fig. 2. Net rectangle of difference approximations for the Box scheme

Now, we consider the net rectangle on the (ξ, η) plane as shown in the Fig. 2 and denote the net points by

$$\begin{aligned} &\xi^0 = 0, \xi^n = \xi^{n-1} + k_n, \\ &n = 1,2,3,---,N \text{ and } \eta_0 = 0, \\ &\eta_j = \eta_{j-1} + h_j,\ j = 1,2,3,---,J \end{aligned} \quad (25)$$

Here, n and j are just the sequence of numbers on the (ξ, η) plane, having k_n and h_j as the variable mesh widths. Now approximating the quantities *f*, *u*, *v* and p , at the points

$\left(\xi^n, \eta_j\right)$ of the net by $f_j^n,\ u_j^n,\ v_j^n,\ p_j^n$ leads to something being termed as net function. It is also employed so that the notation P_j^n for the quantities midways between net points as shown in Fig. 2 and for any net functions as

$$\xi^{n-\frac{1}{2}} = \frac{1}{2}\left(\xi^n + \xi^{n-1}\right) \tag{26}$$

$$\eta_{j-\frac{1}{2}} = \frac{1}{2}\left(\eta_j + \eta_{j-\frac{1}{2}}\right) \tag{27}$$

$$g_j^{n-\frac{1}{2}} = \frac{1}{2}\left(g_j^n + g_j^{n-1}\right) \tag{28}$$

The finite difference approximation according to box method to the three first-order ordinary differential equations (18)-(20) is written for the midpoint
of the $\left(\xi^n, \eta_{j-\frac{1}{2}}\right)$ segment A_1A_2 as shown in Fig. 2.

$$\frac{f_j^n - f_{j-1}^n}{h_j} = u_{j-\frac{1}{2}}^n = \frac{u_{j-1}^n + u_j^n}{2} \tag{29}$$

$$\frac{u_j^n - u_{j-1}^n}{h_j} = v_{j-\frac{1}{2}}^n = \frac{v_j^n + v_{j-1}^n}{2} \tag{30}$$

$$\frac{g_j^n - g_{j-1}^n}{h_j} = p_{j-\frac{1}{2}}^n = \frac{p_j^n + p_{j-1}^n}{2} \tag{31}$$

The finite difference approximation to the first order differential equation (21) and (22) is written for the midpoint $\left(\xi^{n-\frac{1}{2}}, \eta_{j-\frac{1}{2}}\right)$ of the rectangle $A_1A_2A_3A_4$. This procedure yields

$$\begin{aligned}
&\frac{1}{2}\left(\frac{v_j^n - v_{j-1}^n}{h_j}\right) + \frac{1}{2}\left(\frac{v_j^{n-1} - v_{j-1}^{n-1}}{h_j}\right) \\
&+\left(P_1 f\ v\right)_{j-\frac{1}{2}}^{n-\frac{1}{2}} - \left(P_2 u^2\right)_{j-\frac{1}{2}}^{n-\frac{1}{2}} - \left(P_3 u\right)_{j-1/2}^{n-1/2} + g_{j-\frac{1}{2}}^{n-\frac{1}{2}} \\
&= \xi_{j-\frac{1}{2}}^{n-\frac{1}{2}} \begin{pmatrix} u_{j-\frac{1}{2}}^{n-\frac{1}{2}} \dfrac{u_{j-\frac{1}{2}}^n - u_{j-\frac{1}{2}}^{n-1}}{k_n} \\ -v_{j-\frac{1}{2}}^{n-\frac{1}{2}} \dfrac{f_{j-\frac{1}{2}}^n - f_{j-\frac{1}{2}}^{n-1}}{k_n} \end{pmatrix}
\end{aligned} \tag{32}$$

The above equations are to be linearized using Newton's Quasi-linearization method. Then linear

$$\begin{aligned}
&\frac{1}{2\,\mathrm{Pr}}\left(\frac{p_j^n - p_{j-1}^n}{h_j}\right) + \frac{1}{2\,\mathrm{Pr}}\left(\frac{p_j^{n-1} - p_{j-1}^{n-1}}{h_j}\right) \\
&+\left(P_1 f\ p\right)_{j-\frac{1}{2}}^{n-\frac{1}{2}} - \left(P_4 ug\right)_{j-\frac{1}{2}}^{n-\frac{1}{2}} \\
&+\left(P_5\, u^2\right)_{j-\frac{1}{2}}^{n-\frac{1}{2}} + \left(P_6\ g\right)_{j-\frac{1}{2}}^{n-\frac{1}{2}} \\
&= \xi_{j-\frac{1}{2}}^{n-\frac{1}{2}} \begin{pmatrix} u_{j-\frac{1}{2}}^{n-\frac{1}{2}} \dfrac{g_{j-\frac{1}{2}}^n - g_{j-\frac{1}{2}}^{n-1}}{k_n} \\ -p_{j-\frac{1}{2}}^{n-\frac{1}{2}} \dfrac{f_{j-\frac{1}{2}}^n - f_{j-\frac{1}{2}}^{n-1}}{k_n} \end{pmatrix}
\end{aligned} \tag{33}$$

algebraic equations can be rewritten in block matrix that forms a coefficient matrix. The whole methodology which involves mainly reduction to first order pursued by central difference approximations, Newton's Quasi-linearization method and the block Thomas algorithm, is established as the Keller-box method.

5. RESULTS AND DISCUSSION

Here, we have investigated the problem of the steady two dimensional laminar natural convection boundary layer flow of a viscous incompressible electrically conducting fluid along a side of a vertical flat plate of thickness '*b*' insulated on the edges with temperature T_b being maintained on the other side in the presence of a uniformly distributed transverse magnetic field and heat generation. Solutions are obtained for the fluid having Prandtl number *Pr* = 0.01, 0.10 0.72, 1.00, 1.74 and for overall of the Joule heating parameter *Jul* = 0.20, 0.40, 0.70, 0.90 and the heat generation parameter *Q* = 0.10, 0.50, 0.80, 1.10. Also, we consider the controlling magnetic Parameter value only *M* = 1.00, here no variation is not included.

Fig. 3 (a) and 3(b) represent the velocity and the temperature profiles for various values of the Joule heating parameter *Jul* for particular values of the Prandtl's number *Pr* = 0.72, the magnetic parameter *M* = 1.00 and heat generation parameter *Q* = 0.60. From Fig. 3(a), it is perceived that an enhancement in the Joule heating parameter *Jul* is associated with a considerable increase in velocity profiles, but close to the surface of the plate, the velocity increases and becomes maximum and then reduces and finally approaches to zero asymptotically. However, Fig. 3(b) exhibits the

distribution of the temperature profiles against η for some values of the Joule heating parameter *Jul* (=0.90, 0.70, 0.40, 0.20). It is clearly seen that the temperature distribution increases owing to increasing values of Joule heating parameter *Jul* and the maximum is adjacent to the plate wall. The local maximum values of temperature profiles are 1.7662, 1.6886, 1.6164, 1.5496 for *Jul* = 0.90, 0.70, 0.40, 0.20 respectively and each of which attains at the surface. Thus the temperature profiles increase 13.98% as Jul increases from 0.20 to 0.90.

Figs. 4(a) and 4(b) exhibit results for velocity and temperature profiles, for various small values of heat generation parameter, *Q* =0.20, 0.40, 0.70, 0.90 being plotted against η at *Pr* = 0.72, *M* = 1.00 and *Jul* = 0.50. From Fig. 4(a), it is revealed that the velocity profiles $f'(\xi,\eta)$ increases very slightly with the increase in the heat generation parameter, *Q*. In other words, it indicates that heat generation parameter increases the fluid motion slowly. From Fig. 4(b), it is observed that temperature profiles $\theta(\xi,\eta)$ increase for the growing values of heat generation parameter *Q* significantly.

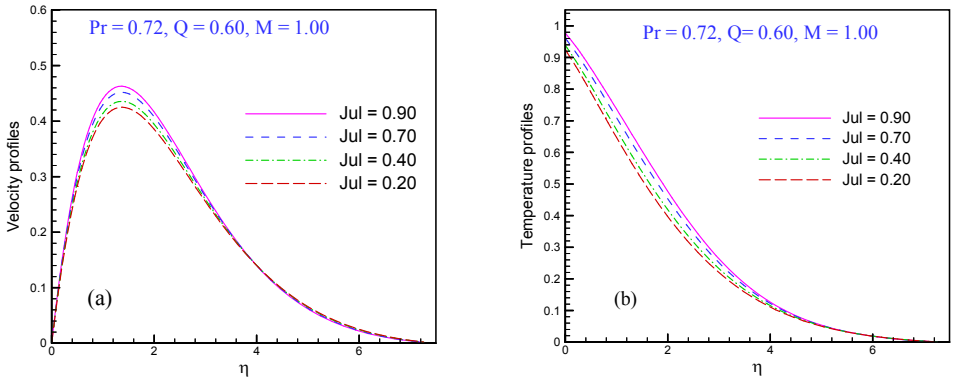

Fig. 3(a) and Fig. 3(b) variation of dimensionless velocity profiles $f'(\xi,\eta)$ and temperature profiles $\theta(\xi,\eta)$ against dimensionless distance η for different values of Joule heating parameters *Jul* with *Pr* = 0.72, *M* = 1.00 and *Q* = 0 .60

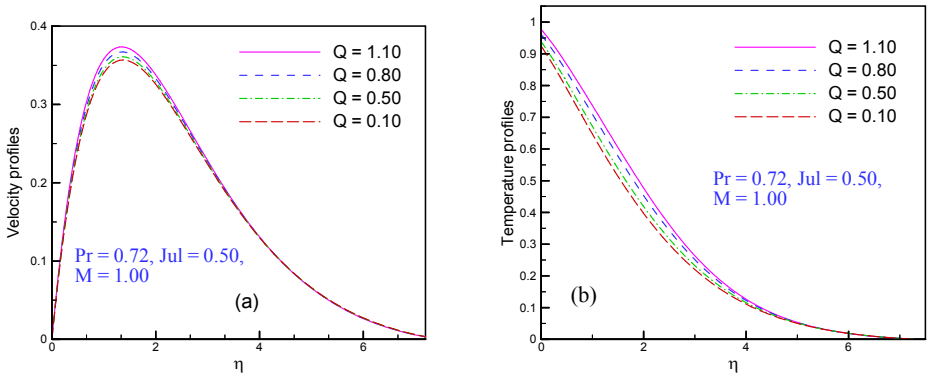

Fig. 4(a) and Fig. 4(b) variation of dimensionless velocity profiles $f'(\xi,\eta)$ and temperature profiles $\theta(\xi,\eta)$ against dimensionless distance η for distinct values of heat generation parameters *Q* with *Pr* = 0.72, *M* = 1.00 and *Jul* = 0 .50

Figs. 5(a) and 5(b) exhibit the outcomes for the velocity and temperature profiles, for different small values of Prandtl's number *Pr* (=1.74, 1.00, 0.72, 0.10, 0.01) being plotted against η at *Jul*=0.60 *M* = 1.00 and *Q* = 0.40. It is observed from Fig. 5(a) that the velocity profile is affected notably and decreases as the value of Prandtl's number *Pr* increases. But near the surface of the plate velocity rises significantly and then falls slowly and lastly approaches to zero. Also, it has been evident that the temperature field decreases with increasing values of Prandtl's number *Pr* in Fig. 5(b).

Numerical values of the velocity gradient and the surface temperature are depicted graphically in Fig.6 (a) and 6(b) respectively against the axial distance in the interval [0, 6.4] for different values of Joule heating parameter Jul (= 0.90, 0.70, 0.40, 0.20). It is seen from Fig. 6(a) that the skin-friction coefficient increases when the Joule heating parameter Jul increases. It is also observed in Fig.6(b) that the surface temperature distribution increases when Jul increases.

Figs. 7(a) and 7(b) illustrate the variation of skin-friction $f''(\xi,0)$ and surface temperature distribution $\theta(\xi,0)$ against ξ for simultaneous values of heat generation parameter *Q* (= 1.10, 0.80, 0.50, 0.10). It is seen from Fig. 7(a) that the skin-friction $f''(\xi,0)$ increases when the heat

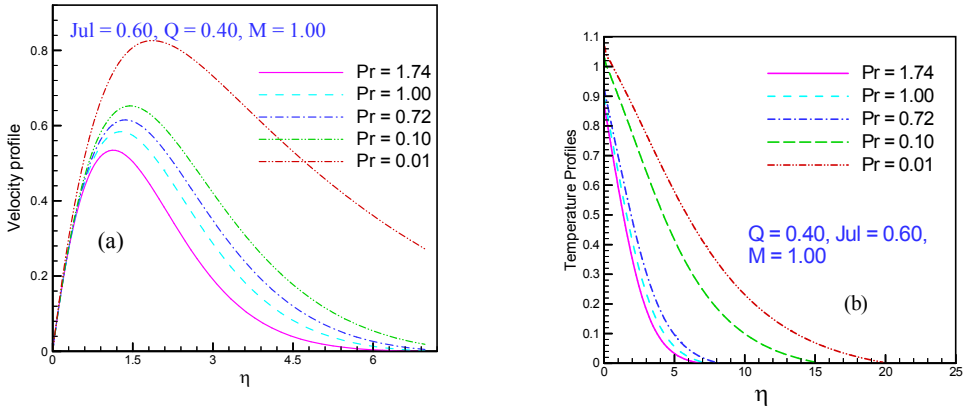

Fig. 5(a) and Fig. 5(b): Variation of dimensionless velocity profiles $f'(\xi,\eta)$ and temperature profiles $\theta(\xi,\eta)$ against dimensionless distance η for different values of Prandtl's number parameters *Pr* with *Q* = 0.40, *M* = 1.00 and *Jul* = 0 .60

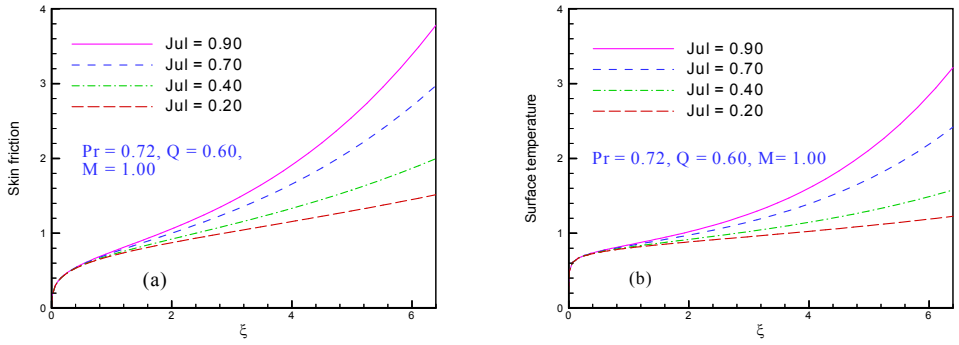

Fig. 6(*a*) and Fig. 6(b): Variation of skin friction coefficient $f''(\xi,0)$ and surface temperature $\theta(\xi,0)$ with dimensionless distance ξ for different values of Joule heating parameters with *Pr* = 0.72, *M* = 1.00 and *Q* = 0 .60

generation parameter *Q* increases. It is also observed from Fig.8 (b) that the surface temperature $\theta(\xi,0)$ distribution increases as *Q* increases. In Fig.8(a), the shear stress coefficient $f''(\xi,0)$ and Fig.8(b), the surface temperature $\theta(\xi,0)$ are presented graphically for different values of the Prandtl's number *Pr* (=0.01, 0.10, 0.72, 1.00, 1.74) when other values of the controlling parameter *Jul* = 0.60, *M* = 1.00 and *Q* = 0.40. Here we take Pr = 0.72 for air, Pr = 1.00 for the electrolyte solutions such as salt water and also *Pr* values of (0.01, 0.10, 0.50) have been used theoretically. Here, it is found that the skin friction and the surface temperature both decrease with increasing values of Prandtl's number.

In Table 1, skin friction coefficient and surface temperature distribution for various values of heat generation *Q* when *Jul* = 0.50, *M* = 1.00 and *Pr* = 0.72 have been entered. Here, it is found that the values of skin friction decrease at a different position of ξ for heat generation parameter *Q* =0.10, 0.50, 0.80, 1.10. The rate of the skin friction increases by 81.68% as the heat generation parameter *Q* changes from 0.10 to 1.10 at position ξ = 3.0049. Moreover, it is examined that the numerical values of the surface temperature distribution increase with rising values of heat generation parameter *Q*. The rate of increase in surface temperature distribution is 54.26% at position ξ = 3.0049 as the heat generation parameter changes from 0.10 to 1.10.

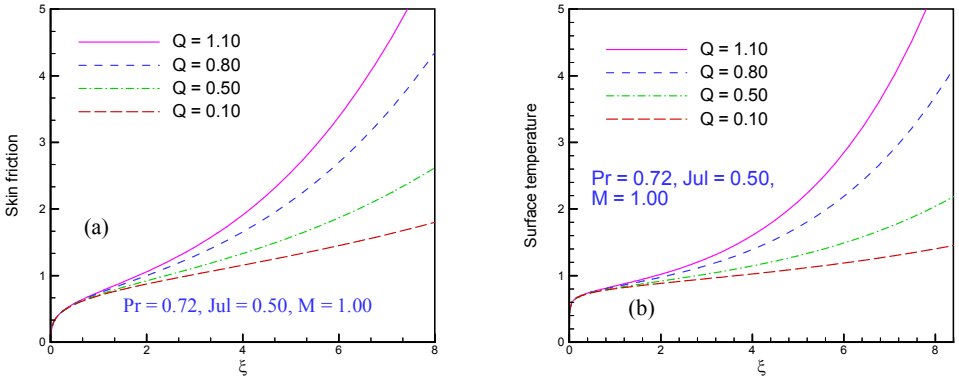

Fig. 7(a) and Fig. 7(b): Variation of skin friction coefficient $f''(\xi,0)$ and surface temperature $\theta(\xi,0)$ with dimensionless distance ξ for various values of heat generation parameters *Q* with *Pr* = 0.72, *M* = 1.00 and *Jul* = 0.50

Table 1. Skin friction coefficient and surface temperature distribution for simultaneous values of heat generation parameter *Q* against ξ with other controlling parameters *Pr* = 0.72, Jul= 0.60

	Q = 0.10		*Q* = 0.50		*Q* = 0.80		*Q* = 1.10	
ξ	$f''(\xi,0)$	$\theta(\xi,0)$	$f''(\xi,0)$	$\theta(\xi,0)$	$f''(\xi,0)$	$\theta(\xi,0)$	$f''(\xi,0)$	$\theta(\xi,0)$
0.0000	0.0155	0.2052	0.0155	0.2052	0.0155	0.2052	0.0155	0.2052
0.3045	0.5083	0.7352	0.5801	0.8126	0.6663	0.9106	0.7686	1.0338
0.7090	0.6416	0.7907	0.7502	0.8847	0.8851	1.0087	1.0490	1.1701
1.0265	0.7067	0.8152	0.8356	0.9168	0.9982	1.0531	1.1981	1.2332
2.0369	0.8372	0.8614	1.0113	0.9773	1.2373	1.1381	1.5208	1.3559
3.0049	0.9169	0.8885	1.1213	1.0131	1.3913	1.1893	1.7337	1.4311
4.0219	0.9794	0.9095	1.2093	1.0414	1.5169	1.2304	1.9101	1.4924
5.0387	1.0296	0.9263	1.2811	1.0645	1.6211	1.2648	2.0583	1.5443
6.0502	1.0717	0.9405	1.3423	1.0844	1.7111	1.2949	2.1877	1.5903

Table-2. Skin friction coefficient and Surface temperature distribution for different values of Joule heating parameter *Jul* against ξ with other controlling parameters *Pr* = 0.72, *M* = 1.00 and *Q* = 0.60

	Jul = 0.20		Jul = 0.40		Jul = 0.70		Jul = 0.90	
ξ	$f''(\xi,0)$	$\theta(\xi,0)$	$f''(\xi,0)$	$\theta(\xi,0)$	$f''(\xi,0)$	$\theta(\xi,0)$	$f''(\xi,0)$	$\theta(\xi,0)$
0.0000	0.0137	0.1873	0.0137	0.1873	0.0137	0.1873	0.0137	0.1873
0.3045	0.6184	0.8871	0.6356	0.9064	0.6535	0.9270	0.6721	0.9488
0.7090	0.9614	1.1362	0.9990	1.1752	1.0387	1.2170	1.0805	1.2618
1.0265	1.2262	1.3369	1.2819	1.3937	1.3407	1.4549	1.4027	1.5208
2.0369	2.2289	2.1726	2.3586	2.3106	2.4962	2.4605	2.6417	2.6228
3.0049	3.5850	3.4674	3.8199	3.7397	4.0692	4.0360	4.3332	4.3575
4.0219	5.6664	5.7475	6.0662	6.2645	6.4906	6.8279	6.9402	7.4402
5.0387	8.7656	9.6629	9.4141	10.6098	10.1026	11.6428	10.8319	12.7665

In Table-2 skin friction coefficient and surface temperature distribution for different values of Joule heating parameter Jul when Q = 0.60, M = 1.00 and Pr = 0.72 is being entered. Here, it is found that the values of skin friction decrease at a different position of for Joule heating parameter Jul =0.20, 0.40, 0.70, 0.90. The rate of the skin friction increases by 74.82% as the Joule heating parameter Jul changes from 0.20 to 0.90 at position ξ = 3.0049. Moreover, it is observed that the numerical values of the surface temperature distribution increase with growing values of Joule heating parameter Jul. The rate of increase in surface temperature distribution is 56.86% at position ξ = 3.0049 as the Joule heating parameter Jul changes from 0.20 to 0.90.

6. CONCLUSIONS

The upshot of Joule heating parameter *Jul*, the heat generation parameter Q and the Prandtl's number Pr on MHD free convection boundary layer flow along a perpendicular flat plate has been studied introducing a new class of transformations. The transformed non-similar boundary layer governing equations of flow with the boundary conditions based on conduction and convection are numerically solved by using the very efficient implicit finite difference method along with Keller box scheme. From the recent observation, the following conclusions may be drawn:

- The skin friction coefficient, the surface temperature, the velocity and the temperature profiles raise with the increasing values of the Joule heating parameter Jul.
- The skin friction coefficient, the surface temperature, the velocity and the temperature profiles are established to increase with the rising values of the heat generation parameter Q.
- It has been shown that the skin friction coefficient, the surface temperature distribution, the velocity profile, the temperature profiles decreases over the whole boundary layer with the increase in the Prandtl's number *Pr*.

COMPETING INTERESTS

Authors have declared that no competing interests exist.

REFERENCES

1. El-Amin MF. Combined effect of viscous dissipation and Joule heating on MHD forced convection over a nonisothermal horizontal cylinder embedded in a fluid-saturated porous medium, Journal of Magnetism and Magnetic Materials. 2003; 263:337-343.
2. Gebhart B. Effects of viscous dissipation in natural convection. J. of Fluid Mech. 1962; 1:225-232.
3. Alam Md M, Alim MA, Chowdhury Md. MK. Effect of pressure stress work and viscous dissipation in natural convection flow along a vertical flat plate with heat conduction, Journal of Naval Architecture and Marine Engineering. 2006;3(2):69-76.
4. Alim MA. Alam Md. M, Abdullah-Al-Mamun, Joule heating effect on the coupling of conduction with magneto-hydrodynamic free convection flow from a

vertical flat plate, Nonlinear Analysis: Modelling and Control. 2007;12(3):307-316.
5. Vajravelu K, Hadjinicolaou A. Heat transfer in a viscous fluid over a stretching sheet with viscous dissipation and internal heat generation, Int. Comm. Heat Mass Transfer. 1993;20:417-430.
6. Hossain MA. Viscous and joule heating effects on MHD free convection flow with variable plate temperature. Int. J. Heat and Mass Transfer. 1992;35(2):3485-3487.
7. Hossain MA, Molla MM, Yao LS. Natural convection flow along a vertical wavy surface temperature in presence of heat generation/absorption. Int. J. Thermal Science. 2004;43:157-163.
8. Miyamoto M, Sumikawa J, Akiyoshi T, Nakamura T. Effect of axial heat conduction in a vertical flat plate on free convection heat transfer, Int. J. Heat MassTransfer. 1980;23:1545-1533.
9. Molla MM, Taher MA, Chowdhury MMK, Hossain MA. Magneto-hydrodynamic natural convection flow on a sphere in presence of heat generation, Nonlinear Analysis: Modelling and Control. 2005; 10(4):349-363.
10. Pozzi A, Lupo M. The coupling of conduction with laminar natural convection along a flat plate. Int. J. Heat Mass Transfer. 1988;31(9):1807-1814.
11. Keller HB. Numerical methods in boundary layer theory. Annual Rev. Fluid Mech. 1978;10:417-443.
12. Cebeci T, Brashaw P. Physical and computational aspects of convective heat transfer. Spring New York; 1984.
13. Safiqul Islam AKM, Alim MA, Md. Rezaul Karim, Rahman ATMM. Effects of conduction variation on MHD natural convection flow along a vertical flat plate, GANIT J. Bangladesh Math. Soc. 2014;63-73.
14. Chowdhury Md MK, Islam MN, MHD free convection flow of viscoelastic fluid past an infinite porous plate. Heat and Mass Transfer. 2000;36:439-447.
15. Hossain MA. Viscous and joule heating effects on MHD free convection flow with variable plate temperature, Int. J. Heat and Mass Transfer. 1992;35:3485-3487.
16. Hossain MA, Alam KCA, Rees DAS. MHD forced and free convection boundary layer flow along a vertical porous plate, Applied Mechanics and Engineering. 1997;2(1): 33-51.

Peer-review history:
The peer review history for this paper can be accessed here:
http://www.sciencedomain.org/review-history/24214